ELSEVIER

Journal of Nuclear Materials 258–263 (1998) 686–693

journal of nuclear materials

Transmutation of plasma facing materials by the neutron flux in a DT fusion reactor

R. Behrisch [a,*], V. Khripunov [b], R.T. Santoro [b], J.M. Yesil

[a] *Max Planck Institut für Plasmaphysik. Euratom Association, Beltzmanstrasse 2, 85748 Garching, Germany*
[b] *The ITER JCT, Max Planck Institut für Plasmaphysik. 85748 Garching, Germany*

Abstract

The neutron induced transmutations, gas production, activation, atomic displacements and afterheat have been calculated for several potential low- and high-Z first wall materials in a DT fusion reactor. The neutron spectra taken are those calculated for the first wall of the shielding blanket proposed for the International Thermonuclear Experimental Reactor (ITER). For low Z materials the production of hydrogen and helium isotopes dominate, while for high Z materials activation and afterheat dominate. For a total flux of 14.1 MeV neutrons corresponding to a wall load of 1 MW a m^{-2}, the tritium production in a 1 cm thick low Z material layer of the first wall is of the order of $10^{16} - 10^{19}$ cm^{-2}, while the calculated He concentrations are of the order of $\sim 10^{-3}$ per wall atom or 10^{20} cm^{-2}. These gases may modify the thermophysical properties of the wall material.

1. Introduction

In fusion experiments, the materials at the vessel walls facing the hot plasma are modified by several processes [1]. These are implantation of hydrogen isotopes and He atoms [2–5], erosion by sputtering and electrical arcs [6–12], redeposition of the eroded material predominantly at more remote deposition dominated areas [1] and, finally, the deposition of the energy released from the plasma, partly in very short times, such as during ELMS and disruptions [13,14]. The atoms eroded by the plasma from the wall material partly enter the plasma as impurities [15]. For the plasma facing areas of the vessel walls of fusion experiments and future fusion reactors, materials have to be selected so that the influence of these effects on the plasma performance and the degradation of the blanket first wall materials are minimised.

In a DT fusion reactor the first wall materials are additionally degraded by neutron bombardment, i.e. the 14.1 MeV neutrons and the lower energy neutron flux induced during slowing down of the 14.1 MeV neutrons in the blanket. Neutron induced reactions with the atoms of some first wall materials have been calculated with partly different results [16–19]. For a detailed comparison of different potential plasma facing materials the transmutations, gas production, activation and after heat have been calculated in this work, using the new neutron cross section compilation for ITER [20,21].

2. Neutron sources and fluxes in a fusion reactor

In the DT fusion reactions (D + T –> n(14.1 MeV) + ^{4}He (3.5 MeV)), 80% of the energy is released in 14.1 MeV neutrons which leave the plasma and enter the vessel walls. The remaining 20% is given to the 3.5 MeV ^{4}He-particles, which have to be confined for some time to deposit their energy in the plasma for maintaining the plasma temperature and heating the new fuel. At steady state, the ^{4}He has to leave the plasma at the same rate as it is produced [22,23].

For a DT fusion reactor, it is envisioned that the power of the 14.1 MeV neutron current to the blanket first wall will be about 1 MW m^{-2} corresponding to 4.43×10^{17} n m^{-2} s^{-1}. In the following discussions all results of wall material modifications by the neutron

* Corresponding author. Tel.: +49 89 3299 1250; fax: +49 89 3299 1149; e-mail: reb@ipp.mpg.de.

0022-3115/98/$19.00
PII: S0022-3115(98)00249-9

bombardment refer to one full power year (FPY) of reactor operation, i.e. an integral 14.1 MeV neutron current of 1 MW a m^{-2}, or about 1.4×10^{25} n m^{-2}. The high energy neutrons will slow down and deposit their energy in the blanket and shield surrounding the plasma [17–19,24]. During slowing down, the neutrons are randomly scattered, absorbed, or produce secondary neutrons in nuclear reactions. By these processes additional lower energy neutrons are created in a blanket and the plasma facing materials. The intensity and energy distribution of these lower energy neutrons depends especially on the distribution of low Z elements in the structure of the blanket.

The neutron fluxes have been calculated for several fusion reactor designs with different blankets by computer codes simulating the transport of neutrons and photons in the blanket. The total neutron fluxes are typically a factor of 10 higher than the primary neutron current from the plasma. The first wall spectra are similar for different fusion reactor designs.

The neutron spectrum for ITER was calculated using two dimensional discrete ordinate methods [21,29]. The ITER first wall is comprised of a 1-cm-thick Be layer bonded to a 2 cm thick water-cooled Cu heat sink that is fixed to a 2-cm-thick stainless steel layer which is mounted to the water-cooled shielding blanket. The combined thickness of the shielding blanket and vacuum vessel is about 1 m. The neutron spectrum calculated in the plasma facing first wall is shown in Fig. 1. This neutron flux energy distribution is used for calculating the modifications of different 1 cm thick plasma facing materials. For plasma facing materials containing elements with a large neutron cross section at some energy, the neutron spectrum used here becomes depleted at this energy. This is not included in these calculations.

3. First wall materials

For the plasma facing areas, materials with a low atomic number Z are strongly favoured. Low Z atoms cause much lower radiation losses in the plasma than high Z atoms and higher concentrations can be tolerated in a burning plasma [15]. The materials widely used in today's plasma experiments are Be, fine grain graphite, carbon fibre enforced carbon, and doped graphites mostly with carbides, such as B_4C, TiC, SiC. These materials are also favoured for ITER [25–27,30]. However, some materials with atoms of a high atomic number Z, such as Mo, W, Re have a much lower erosion rate and a higher threshold energy for sputtering than the low Z materials [7–9]. If the plasma temperature close to the plasma facing materials can be sufficiently decreased, these materials are also of interest [25,30–32]. Therefore, the neutron induced modifications of both low Z materials as well as of some high Z materials are calculated in this work. Finally some elements, which have been found as major impurities at levels in the few percent range in the surface layers of today's fusion experiments, such as O, N, Cl [10,33] are also included.

4. Neutron induced processes

The major neutron induced processes causing a modification of the plasma facing material are:

1. Transmutations of the atoms of the materials by nuclear reactions leading to loss of the elements, includ-

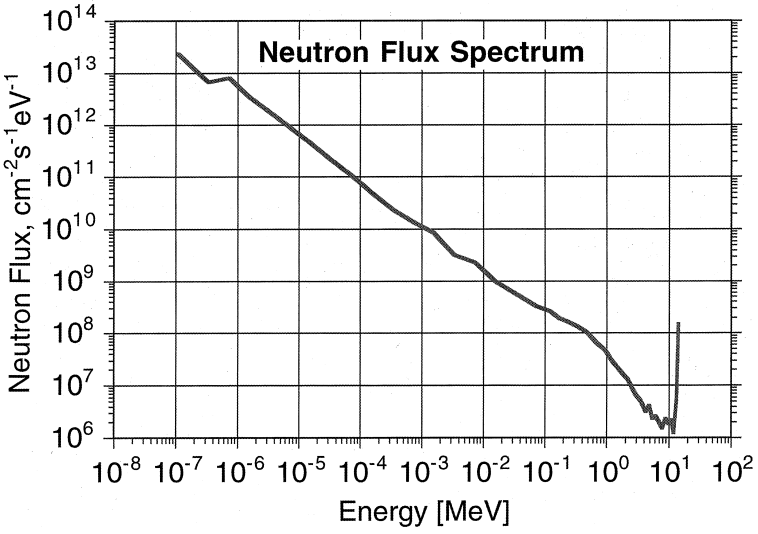

Fig. 1. Neutron spectrum calculated at the ITER first wall.

ing hydrogen and helium gas production and activation of the material.

2. Atomic displacements, leading to lattice disorders, i.e. creation of Frenkel defects which may anneal at elevated temperature or form larger defect clusters. The damage sites may further be traps for the gases produced.

All these processes generally enhance the degradation of the thermo-physical and mechanical properties of the plasma facing wall materials.

5. Cross sections and neutron group fluxes

The cross sections for the different neutron induced processes depend largely on the neutron energy. They have been collected at different places and the data have been re-evaluated for the ITER predictions [20,21]. For the neutron transport calculations [29] and for the neutron induced activation calculations [34] for the materials studied here the neutron spectrum (Fig. 1) and cross sections were represented in 175 energy intervals or groups $\Delta E_v = E_{2v} - E_{1v}$, with E_{1v} and E_{2v} being the lower and upper energy limits of the groups with intensity $\phi(E_v)\Delta E_v$, (Fig. 2(a)).The group structure (Fig. 2(a)) is mainly determined by the energy dependence of the cross sections, i.e., the energy intervals where the cross sections are about constant.

The neutron cross sections, $\sigma(E_v)$, in the energy intervals ΔE_v for the major reactions with ^{6}Li, ^{7}Li, ^{9}Be, ^{10}B, ^{12}C and ^{13}C, in which ^{3}H and ^{4}He are produced, are shown in Fig. 2(b). The reaction rates for each energy group, i.e. the products of the neutron flux with the macroscopic cross sections for these reactions are shown in Fig. 2(c), while in Fig. 3 the reaction rates for different larger energy intervals, i.e. the low energies $E \leqslant 0.1$ < MeV, two medium energy ranges 0.1 < MeV $\leqslant E \leqslant 2$ MeV, and 2 MeV $\leqslant E \leqslant 12$ MeV and the highest energies 12 MeV $\leqslant E \leqslant 14.5$ MeV are shown. For the ^{6}Li (n,T)^{4}He and the ^{10}B(n,α)^{7}Li reactions, the cross sections increase with decreasing neutron energy (see Fig. 2(a)) and this shows up in the major contributions of low energy neutrons to transmutations and gas production. For Be and C the major contributions to transmutations come from high energy neutrons, i.e. $E > 2$ MeV.

The total reaction probabilities for different wall atoms can finally be obtained by adding the reaction probabilities for all energy groups. In the following, the total reaction probabilities have, however, been calculated directly for one FPY of operation with the FISPACT code [34] for 1-cm-thick layers of each material for the neutron flux obtained for the plasma facing material of ITER (Fig. 1 and Fig. 2(a)). In these calculations, the continuous modification of the composition of the material and the decay of transmuted wall atoms is included. The transmutation probabilities, gas production, displacement damage, after heat, and radioactivity per first wall atom after one FPY, immediately after shut down, are shown in Figs. 4–7.

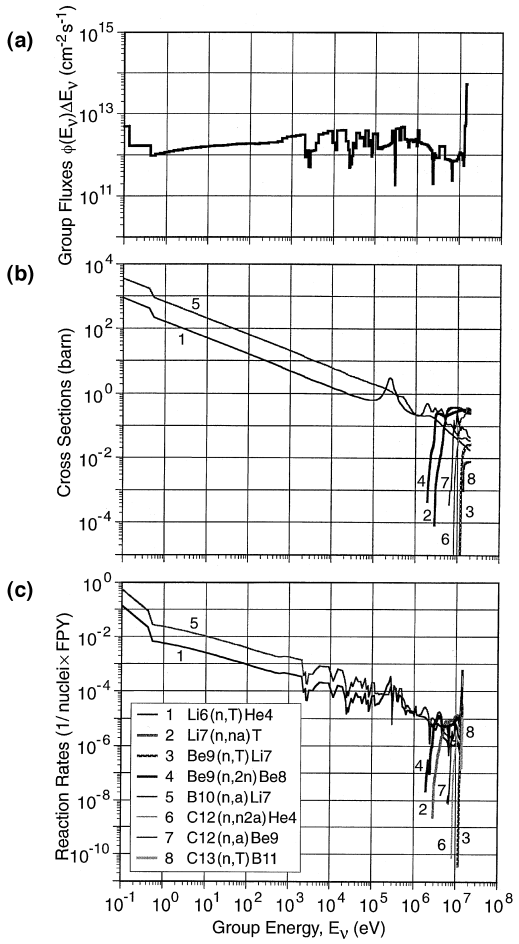

Fig. 2. (a) Neutron fluxes integrated over energy groups; (b) Cross sections for the neutron reactions for several low Z elements [20,21]; (c) Neutron reactions for the different energy groups, i.e. the product of the group neutron fluxes and the cross sections.

6. Results

6.1. Transmutations and gas production

For the majority of elements considered here, the transmutation probabilities (Fig. 4) are in the 10^{-3} range, except for ^{6}Li, ^{10}B, N, Cl, the medium Z elements V, Ni, and Cu, and the high Z elements Ga, Mo, Ta, W, and Re. For the low Z elements of high interest, i.e. ^{9}Be, C, and B(nat.) the transmutation probabilities after one FPY of operation are 10^{-3}, 7×10^{-4}, and 0.12, respec-

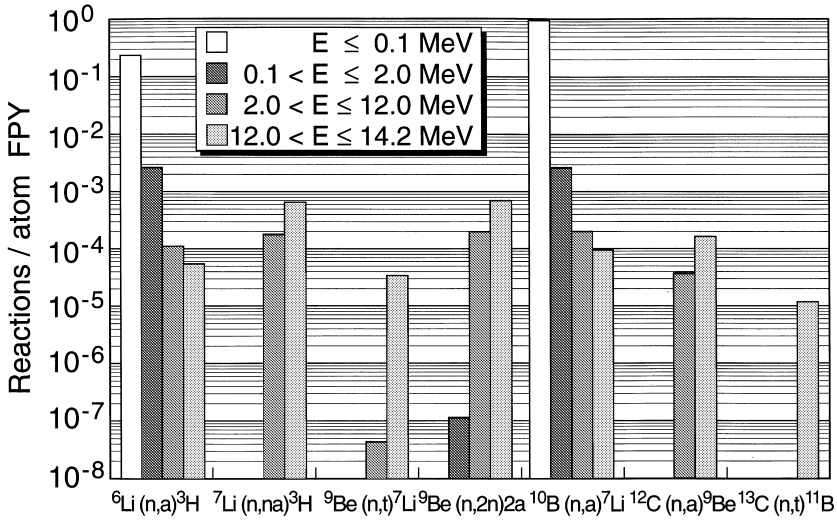

Fig. 3. Reaction probabilities for ^{6}Li, ^{7}Li, ^{9}Be, ^{10}B, ^{12}C, and ^{13}C with the neutrons of four energy ranges after one FPY.

tively. For B, the major contribution originates from ^{10}B where more than one half is lost after one FPY, while for ^{11}B only about 10^{-4} is transmuted. ^{3}He has a very large probability of 0.7, for transmutation to tritium and hydrogen.

For the low Z elements, hydrogen and helium gas production dominates. ^{9}Be is mostly transmuted to two ^{4}He atoms in ^{9}Be(n,2n)^{8}Be $\rightarrow$ 2 ^{4}He reactions, while the probability for tritium production in ^{9}Be(n,^{3}H)^{7}Li reaction is 5×10^{-4}/FPY. The second reaction product, ^{7}Li, is finally also transmuted to tritium and ^{4}He. The ^{12}C is transmuted to ^{4}He and ^{9}Be, while ^{13}C is transmuted to tritium and ^{11}B. This means that in natural C some ^{3}H is also produced with a probability of about 1.5×10^{-7}/FPY. The largest tritium production occurs for ^{6}Li (Li nat.) and ^{10}B (B nat.) where the probabilities for on FPY are 0.2 (1.8×10^{-2}) and 5×10^{-4} (1.4×10^{-4}), respectively. Tritium production for the high Z materials is in the 10^{-7} FPY region. Protium production is in 10^{-5} – 10^{-3} range for the elements regarded here, while ^{4}He production decreases from above 10^{-1} to about 10^{-5} in going from low Z to high Z elements, and ^{3}He production is mostly more than 2 orders of magnitude below ^{4}He production (Fig. 4).

The relatively large amount of helium and hydrogen will mostly be trapped in the materials, preferentially at damage sites, leading to a decrease of the thermophysical properties of the materials, including the thermal conductivity [28].

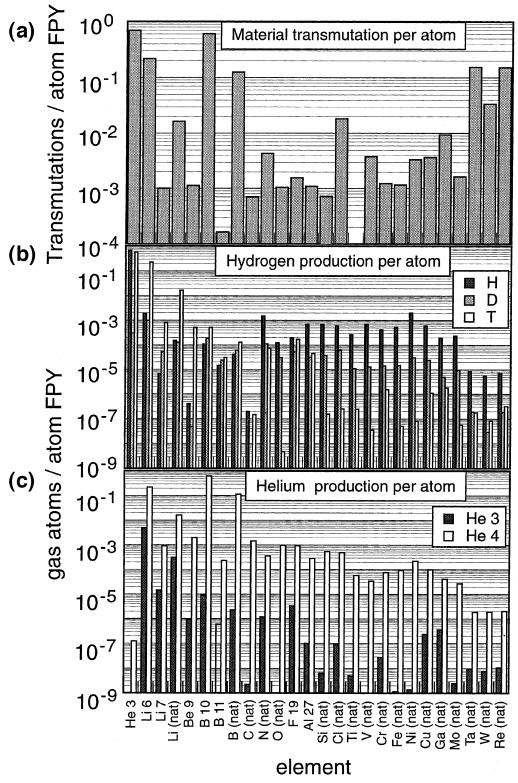

Fig. 4. (a) Fraction of transmuted atoms for different first wall materials after one FPY of reactor operation; (b) produced hydrogen isotopes per atom and (c) produced helium isotopes per atom.

6.2. Damage and Afterheat

The primary recoils produced by the neutron impact on the materials initiate atomic collision cascades in the solid which cause displacement damage in the crystallites. The damage is generally measured by displacements per atom (DPA), defined as the average

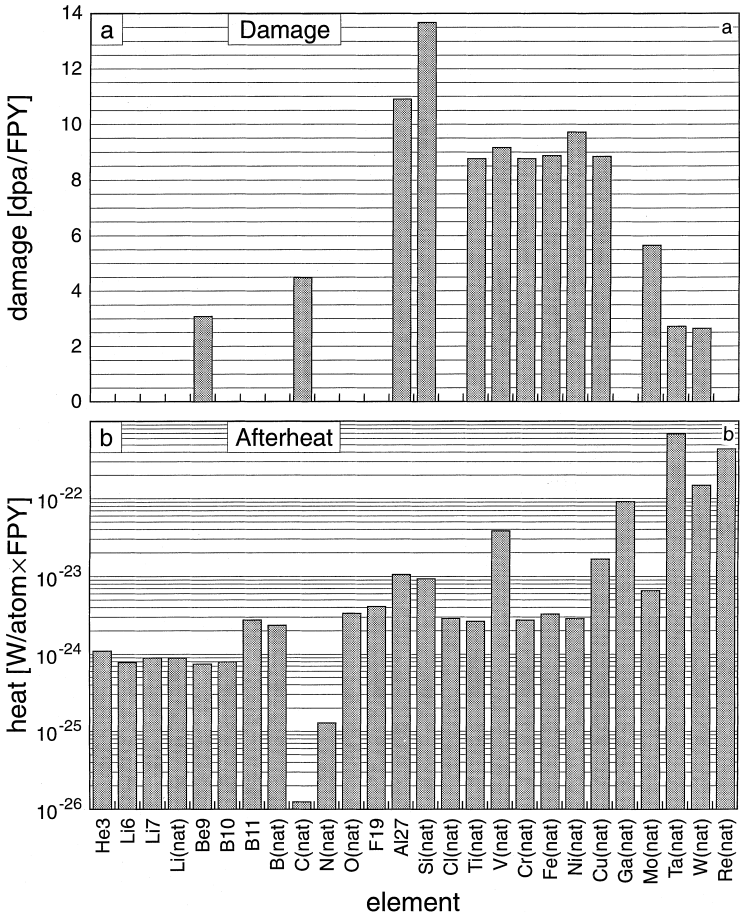

Fig. 5. (a) Displacement damage (dpa) and; (b) afterheat (per atom) for several potential first wall materials after one FPY of reactor operation.

number of displacements of every atom in a material. This number, as obtained from the calculations with the DANTSYS code [29], is plotted in Fig. 5(a). For most materials the DPA is about 9 per FPY, while it is about 3 – 4.5 for Be and C. At these DPA levels, degradation of thermal and mechanical properties becomes noticeable. Due to the simultaneous gas production the damage sites will be stabilised by accumulating gas, likely gas bubbles [28]. The gas may also stimulate the growth of larger voids in a material.

The radioactive decay of transmuted atoms deposits power in the wall materials. This power was also calculated for the time immediately after reactor shut down (Fig. 5(b)). Generally the power is very low and will not present a cooling problem, except for some high Z elements, where values of up to several 10 W/cm^3 FPY are obtained. In the calculations, possible dips in the neutron spectrum have been neglected.

6.3. Radioactivity

A serious problem for maintenance and disposal is the radioactivity induced in the first wall materials by neutrons. The numbers calculated for different pure potential first wall materials for the time immediately after shut down are summarised in Fig. 6. Depending on the half lives of the radioactive nuclei, the activity will decrease with time. For the low Z elements a major contribution is found to originate from the produced tritium which is assumed to be accumulated (at damage sites) in the materials. Tritium under goes ß-decay, with a half life of 12.3 years. For reducing the radioactivity of

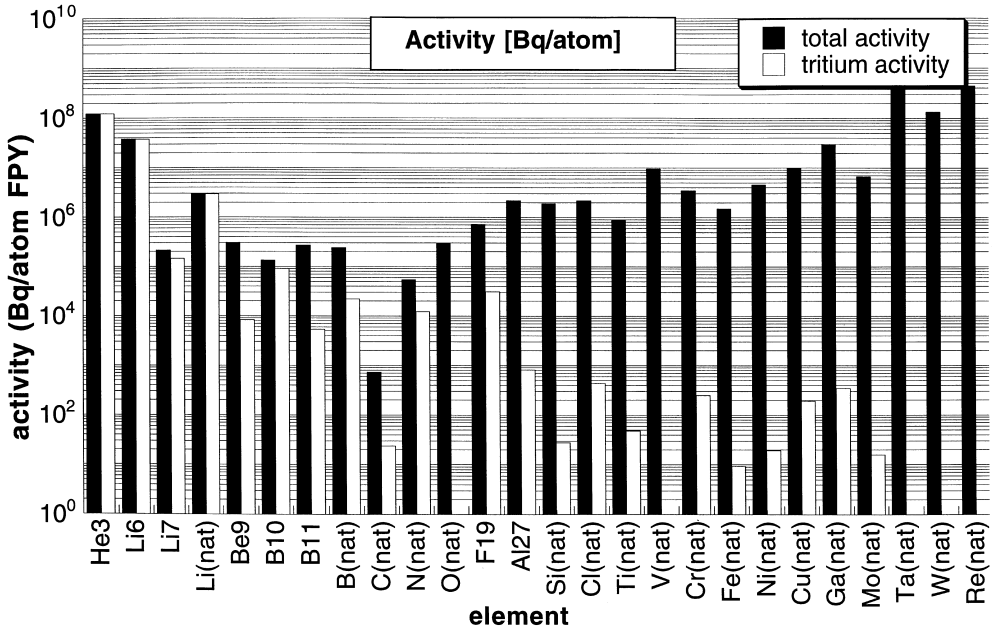

Fig. 6. Radioactivity (total activity by α,β, and γ decay, and due to tritium) of potential first wall materials after one FPY of operation.

the low Z materials, means have to be developed to remove the tritium. Such means are already discussed in relation to remove the tritium "codeposited" on the plasma exposed wall areas. For the medium and high Z elements the major contribution to radioactivity are α- and γ- radiation. The lowest induced radioactivity is found for carbon, while the induced radioactivity is largest for the high Z elements Ta, W and Re.

Finally the reaction products for pure Si, Ti and W calculated for one FPY of operation are shown in Fig. 7. For Si the elements O and F are produced in the 10^{-12} per atom range, while Ne, Mg, Al, Si, P, and S are produced in the $10^{-4} - 10^{-9}$ per atom range. For Ti the elements Ar and K are produced in the $10^{-11} - 10^{-10}$per atom range, and Ca, Sc, V and Cr in the 10^{-5} per atom range. For W isotopes of Hf, Ta, Re, Os are produced in the 10^{-6} to 10^{-4}, and Ir in the 10^{-9} per atom range.

7. Summary and conclusions

The results of the systematic calculations using neutron transport and activation codes, with the most recent, revised data for the neutron cross sections confirmed the dominance of hydrogen and helium gas production for the lower Z materials, while for higher Z atoms transmutations to radioactive nuclei are dominant. In a 1 cm thick Be first wall the tritium production will be about 3.5×10^{18} ^{3}H cm^{-3}, while for C about 10^{17} ^{3}H cm^{-3} and for B_4C about 2×10^{19} ^{3}H cm^{-3} will be produced for one FPY of reactor operation. Transmutations in the plasma facing materials are in the 10^{-3} to 10% range and gas production is in the 10^{-5} range for hydrogen, in the 10^{-7} range for tritium, and in the $10^{-4} - 10^{-5}$ range for ^{4}He. The lowest transmutations in the 10^{-4} range are found for C and Ti.

The radioactivity induced by the neutron bombardment in pure lower Z elements after one full power operation year is mostly due to the tritium, while for higher Z elements the α- and γ-radiation of the transmuted atoms dominate. The very low induced radioactivity, i.e. below 10^{-14} Bq per carbon atom is again confirmed, while the high Z elements exhibit the highest induced radioactivity of up to 10^{-8} Bq per atom.

The decay heat is in the 0.1 W/cm^3 range for the low Z elements and should not cause problems. For Ga, Ta, W and Re it will be in the several 10 W/m^3 range after shut down and active cooling of the reactor may be necessary.

These neutronic investigations of several potential first wall materials show advantages for low Z materials, such as Be, ^{11}B and C with respect to transmutations afterheat and induced radioactivity, compared to the high Z materials Ta, W, and Re. Among the medium Z

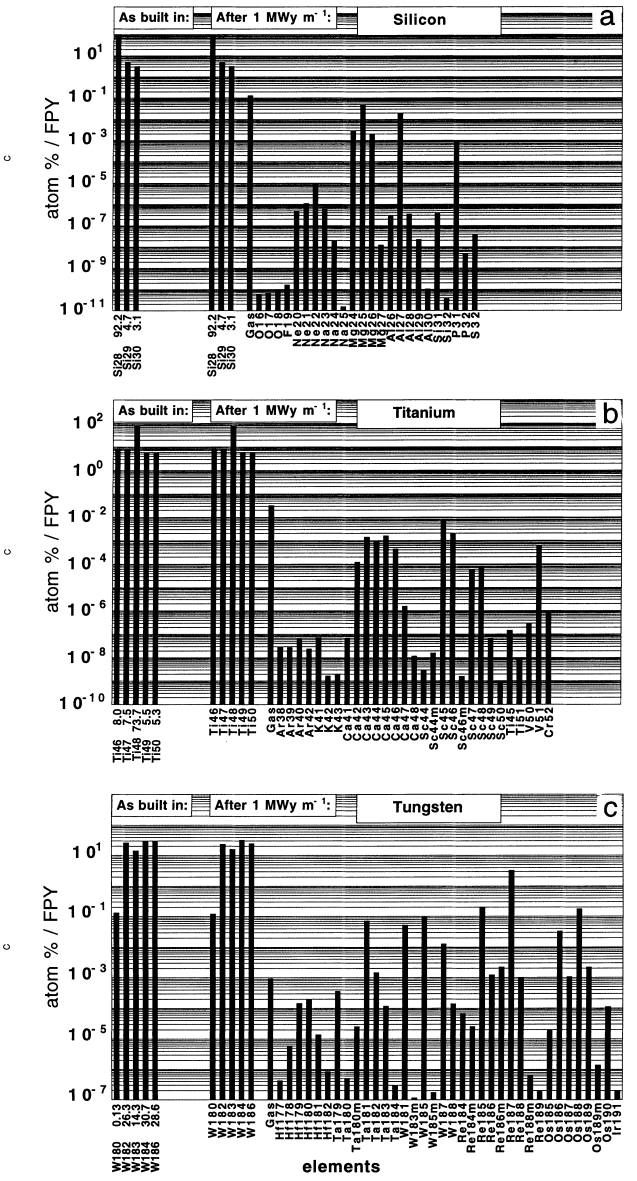

Fig. 7. Reaction products for pure Si, Ti, and W after one FPY of reactor operation. At the start, the natural isotope composition is taken, shown at the left side.

materials Ti shows reasonable performance, especially with respect to transmutations.

References

[1] R. Behrisch, M. Mayer, C. García-Rosales, J. Nucl. Materials 233–237 (1966) 673.
[2] R. Behrisch, J. Ehrenberg, J. Nucl. Materials 155–157 (1988) 95.
[3] G. Sun, M. Friedrich, R. Grötzschel, W. Bürger, R. Behrisch, C. García-Rosales, J. Nucl. Materials 246 (1997) 9.
[4] P. Franzen, R. Behrisch, C. García-Rosales, The ASDEX-Upgrade team, in: D. Schleussner, D. Rösler, J. Becker, W. Knapp, Ch. Edelmann (Eds.), Nuclear Fusion, 37 (10), 1997, p. 1375.
[5] G. Federici et al., ISFNT-4, Fusion Eng. and Design, 1997.
[6] R. Behrisch, Nuclear Fusion 12 (1972) 691.
[7] R. Behrisch (Ed.), Sputtering by Particle Bombardment I, Topics in Applied Physics, Springer, Berlin, vol. 47, 1981.
[8] J. Roth, Physics of Plasma–Wall Interactions in Controlled Fusion, in: D.E. Post, R. Behrisch (Eds.), NATO ASI Series, Plenum Press, New York, 1986, p. 351.
[9] C. García Rosales, J. Nucl. Materials 212 (1994) 97.
[10] M. Mayer, R. Behrisch J. Nucl. Materials 241–243 (1997).

[11] R. Behrisch, Physics of plasma–wall interactions in controlled fusion, in: D.E. Post, R. Behrisch (Eds.), NATO ASI Series, Plenum Press, New York, 1986, p. 495.
[12] C. García Rosales, R. Behrisch, D. Hildebrandt, B. Jüttner, W. Schneider, H. Wolff, ASDEX-upgrade team, Proc. 21. EPS conference on controlled fusion and plasma physics, Europhysics Conference Abstracts, Vol 18B/II, 1994, 718.
[13] J. Lingertat, A. Tabasso, S. Ali-Arshad et al., J. Nucl. Materials 241–243 (1997) 402.
[14] E. Gauthier, Proc. 24. EPS conference on controlled fusion and plasma physics, Europhysics Conference Abstracts, 18B/II (1997) 718.
[15] J.L. Checci, J. Nucl. Materials 93&94 (1980) 28.
[16] G.M. McCracken, G. Constantine, Proceedings of the 18th Symposium on Fusion Technology (SOTF), Jutphas 1974, EUR 5183, 1976.
[17] G.R. Hopkins, R.J. Price, Nucl. Eng. and Design/Fusion 2 (1985) 111.
[18] H. Bolt, Fusion Eng. and Design 22 (1993) 89.
[19] G.R. Longhurst, Idahoe National Engineering and Environmental Laboratory, Report ITER/US/95/TE/SA-7, 1997.
[20] IAEA Specialist Meeting on the Fusion Evaluated Nuclear Data Library (FENDL), Vienna, Austria, 1994, IAEA Nuclear Data Section Report INDC (NDC)-312, 1994.
[21] A.B. Pashenko, Compilation of FENDL-1 and START FENDL-2, IAEA Report INDC (INS)-352, 1996.
[22] D. Reiter, G.H. Wolf, H. Klever, Nuclear Fusion 30 (1990) 2141.
[23] R. Behrisch, V. Prozesky, Nuclear Fusion 30 (1990) 2166.
[24] Technical basis for the ITER interim design report, Cost review and Safety Analysis, ITER EDA Documentation Series, No. 7, IAEA, 1996.
[25] G. Janeschitz, J. Nucl. Materials 220/222 (1995) 73.
[26] R. Matera et al., J. Nucl. Materials 233-237 (1996) 17.
[27] R. Parker, G. Janeschitz, H.D. Pacher, D. Post, S. Chioco, G. Federici, P. Ladd, ITER joint central team and home teams, J. Nucl. Materials 241–243 (1997) 1.
[28] P. Jung, Diffusion Processes in Nuclear Materials, in: R.P. Agarwala (Ed.), Elsevier, Amsterdam, 1992, p. 235.
[29] R.E. Alcouffe, R.S. Baker et al., DANTSYS 3.0 One-, Two-, and Three-Dimensional, Multi-group, Discrete Ordinates Code System. LANL. RSIC Code Package CCC-547, 1995.
[30] V. Barabash, these Proceedings, p. 149.
[31] D. Düchs, G. Haas, D. Pfirsch, H. Vernickel, J. Nucl. Materials 53 (1974) 102.
[32] D. Naujoks, K. Asmussen, M. Bessenrodt–Weberpals et al., Nuclear Fusion 36 (1996) 617.
[33] A. Martinelli et al., J. Nucl. Materials 212 (1994) 97.
[34] R.A. Forrest, J.-Ch. Sublet, FISPACT user manual, EASY Documentation Series, UKAEA FUS 287, 1995.